Preprints (www.preprints.org) | NOT PEER-REVIEWED | Posted: 18 January 2019 doi:10.20944/preprints201901.0183.v1

Peer-reviewed version available at Electronics 2019, 8, 172; doi:10.3390/electronics8020172

# An experimental study of the failure mode of ZnO varistors under multiple lightning stroke

Chunlong ZHANG[1,2,3,4], Hongyan XING[1,2,3,*], Pengfei LI[4], Chunying LI[4], Dongbo LV[4], and Shaojie YANG[4]

1 Collaborative Innovation Center on Forecast and Evaluation of Meteorological Disasters, Nanjing University of Information Science & Technology, Nanjing, 210044, China

2 Jiangsu Key Laboratory of Meteorological Observation and Information Processing, Nanjing University of Information Science & Technology, Nanjing, 210044, China

3 School of Atmospheric Physics, Nanjing University of Information Science & Technology, Nanjing, 210044, China

4 Meteorological Disaster Prevention Technology Center of Heilongjiang Province, Harbin, 150030, China

***Corresponding author**

Collaborative Innovation Center on Forecast and Evaluation of Meteorological Disasters, Nanjing University of Information Science & Technology, Nanjing 210044, China.

E-mail: xinghy@nuist.edu.cn



© 2019 by the author(s). Distributed under a Creative Commons CC BY license.

Preprints (www.preprints.org) | NOT PEER-REVIEWED | Posted: 18 January 2019 doi:10.20944/preprints201901.0183.v1

Peer-reviewed version available at Electronics 2019, 8, 172; doi:10.3390/electronics8020172

**ABSTRACT:** In this study, in order to explore the failure mode of ZnO varistors under multiple lightning stroke, a 5-pulse 8/20 μs nominal lightning current with pulse intervals of 50 ms was applied to the ZnO varistors. Scanning electron microscopy (SEM) and X-ray diffractometry (XRD) were used to analyze the microstructure of the material. The failure processes of ZnO varistors caused by multiple lightning impulse current were described. The performance changes of ZnO varistors after multiple lightning impulses were analyzed from macro and micro perspectives. According to the results of this study's experiments, the macroscopic failure mode of the ZnO varistors after multiple lightning impulse was that the electrical parameters deteriorate rapidly with the increase of the number of impulse groups, and finally destroyed by side-corner cracking. The microstructural examination indicated that after the multiple lightning strokes, the proportion of Bi in the several crystal phases had been converted, the grain size of ZnO varistors became smaller, and the white intergranular phase (Bi-rich grain boundary layer) increased significantly. The failure mechanism was thermal damage and grain boundary structure damage caused by temperature gradient thermal stress generated by multiple lightning current.

**KEYWORDS:** failure mode, impulse current, microstructure, multiple lightning, ZnO varistors.

Preprints (www.preprints.org) | NOT PEER-REVIEWED | Posted: 18 January 2019 doi:10.20944/preprints201901.0183.v1

Peer-reviewed version available at Electronics 2019, 8, 172; doi:10.3390/electronics8020172

## 1 Introduction

The installations of surge protective device are one of the most economical and effective means for power distribution systems to avoid or reduce lightning impulse. The core component of a surge protective device is a ZnO varistor, which has many advantages. These include a good nonlinear property, small normal leakage current, low level of residual pressure, and no follow current. ZnO varistors have been widely applied for the protection of electronic and electrical equipment from lightning [1–2]. However, after a natural lightning strike, ZnO varistors often have varying degrees of failure.

Impulse test is the most direct means to study its performance. Currently, an 8/20 μs single pulse waveform had been adopted for the impulse test of ZnO varistors [3–4]. A host of studies have been presented in regard to the performance changes in ZnO varistors under single pulse lightning impulses [5–8]. However, the modern lightning observations and artificial triggered lightning acquisition data have shown that two-thirds of the lightning events in natural settings are multi-pulse processes. According to the statistical data, nearly 70% of cloud-to-ground lightning strikes involve 2 up to 20 strikes, with an average number of between 3 and 5, and the time duration between strikes was 15 ms to 150 ms. There is a significant difference between the single-pulse lightning waveform and the multiple lightning strikes of natural lightning [9–10], and the total time and energy of a multi-pulse is several times that of a single pulse. Therefore, lightning single pulse test methods have been unable to simulate the subsequent damages caused by lightning [11]. Darveniza et al. [12] pointed out that multiple lightning impulse currents could potentially cause severe damage to the lightning protection devices protecting equipment in power distribution systems. The previous research results have shown that 6-pulse lightning current impulses have resulted in serious damage to lightning protection components, and are worthy of

Preprints (www.preprints.org) | NOT PEER-REVIEWED | Posted: 18 January 2019 doi:10.20944/preprints201901.0183.v1

Peer-reviewed version available at Electronics 2019, 8, 172; doi:10.3390/electronics8020172

inconclusion in the lightning protection test standard. Lee et al. [13–14] found that ZnO varistors degraded when subjected to multiple impulse currents, and their life mainly depended on the amplitude of the lightning surge. Haryono et al. [15–16] analyzed the damage effects of ZnO varistors undergoing multiple lightning impulse current from the perspective of energy absorption. At the present time, the research regarding the performances of ZnO varistors undergoing multiple lightning impulse current has been mainly based on the analysis of the macroscopic electrical properties [17–19]. However, few research studies have been conducted to investigate the damage failure mechanisms under multi-pulse continuous impulses, especially in regard to the changes in microstructures.

Therefore, in this study, the samples were applied to a 5-pulse current with a time interval of 50 ms. The actual lightning strike of the ZnO varistors in practical applications was simulated as realistically as possible, and the macroscopic damage form and static parameter variation characteristics were monitored. At the same time, the ZnO varistors before and after the impulse were analyzed by scanning electron microscopy (SEM) and X-ray diffractometry (XRD). It was expected that we would investigate the ZnO varistors' failure mode during natural lightning strikes from the perspective of macroscopic and microscopic bonding. Some experimental data regarding the performance of ZnO varistors under multiple lightning impulse current are shown here. The failure modes of the ZnO varistors undergoing multiple lightning impulse currents are discussed on the basis of the results of thermal effect. It was believed that this was particularly important for improvements in the lightning protection and safety performances of ZnO varistors.

## 2 Experimental

### 2.1 Impulse test and waveform

Preprints (www.preprints.org) | NOT PEER-REVIEWED | Posted: 18 January 2019 doi:10.20944/preprints201901.0183.v1

Peer-reviewed version available at Electronics 2019, 8, 172; doi:10.3390/electronics8020172

The multiple lightning impulse equipment used in this experiment was a 20-pulse lightning impulse current generator, as shown in Fig. 1. Multi-channel discharge technology was adopted to simulate multiple lightning stroke processes. The waveform generator circuit diagram is shown in Fig. 2, where C is the capacitor, G is the impact gap, Rs is the resistor, and Ls is the inductor. With the impulse test end as the axis, there are 10 trigger channels at each end. When the primary current is fully triggered, 20 high-voltage pulses can be generated, and the time interval can be changed from 1 ms to 999 ms.


**Fig. 1** 20-pulse lightning impulse current generator.

Preprints (www.preprints.org) | NOT PEER-REVIEWED | Posted: 18 January 2019 doi:10.20944/preprints201901.0183.v1

Peer-reviewed version available at Electronics 2019, 8, 172; doi:10.3390/electronics8020172

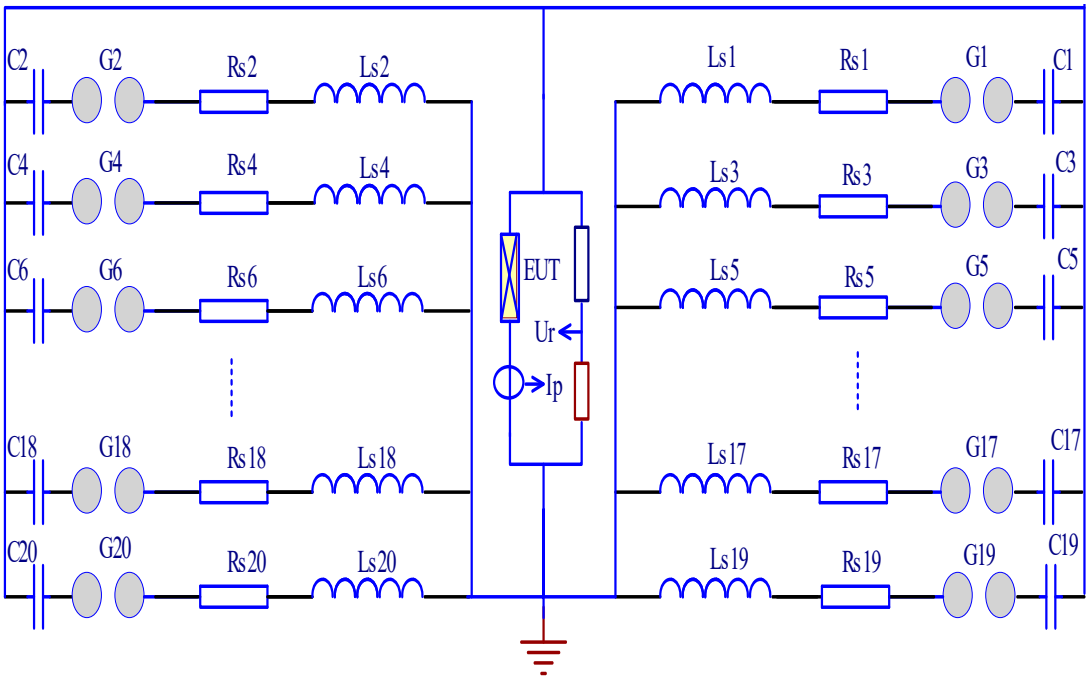


**Fig. 2** Multiple lightning impulse current generator circuit diagram.

In this study, section 1 of IEC 62305-1 Lightning Protection: General Rule [20] provides a special definition for the multiple lightning. Lightning with an average of 3 to 4 impulses, and intervals of approximately 50 ms, was defined as multiple lightning. Therefore, the multiple lightning strikes in this test were represented by a group of multiple impulse currents that was used, which included five consecutive impulse currents, each of which had 8/20 μs waveforms, the time between two consecutive pulses was 50 ms, and the pulse amplitudes were the nominal discharge currents of the selected ZnO varistors. The waveform diagram is shown in Fig. 3, where the five yellow vertical lines represent the five pulses, and the following 8/20 μs waveform denotes the full waveform figure of a single pulse.

Preprints (www.preprints.org) | NOT PEER-REVIEWED | Posted: 18 January 2019 doi:10.20944/preprints201901.0183.v1

Peer-reviewed version available at Electronics 2019, 8, 172; doi:10.3390/electronics8020172

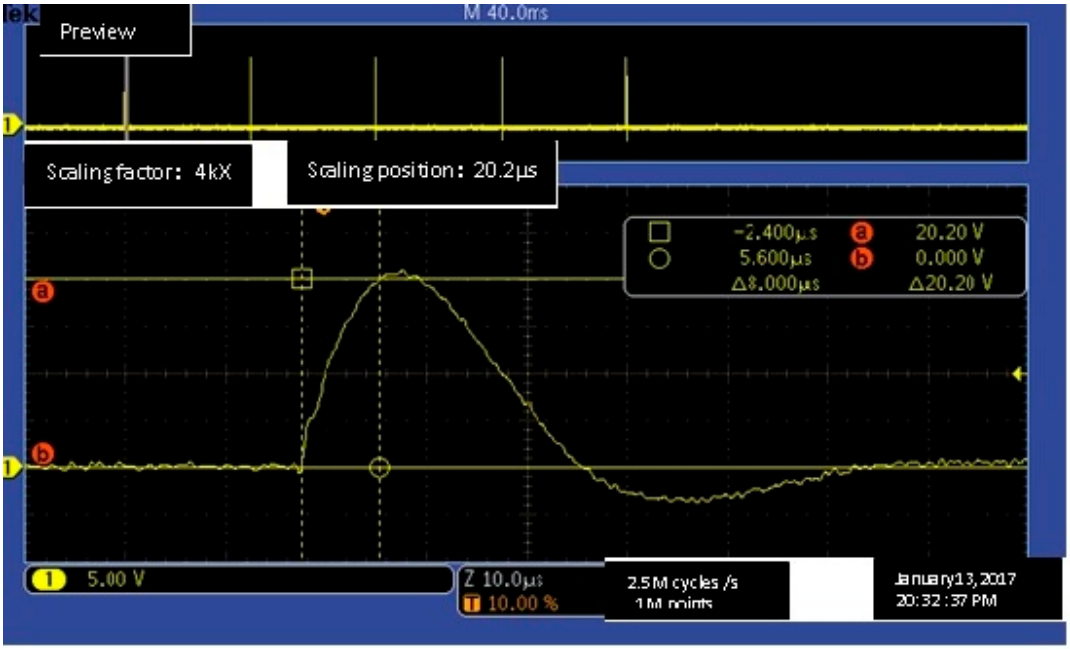


**Fig. 3** 5-pulse lightning waveform diagram.

### 2.2 Sample preparation

In this study, the same type of ZnO varistors that were used in this experiment were provided by the same manufacturer. The basic parameters of these samples were nominal discharge current In = 20 kA, maximum continuous operation voltage Uc = 385 V, and the static parameters (varistor voltage and leakage current) were as shown in Table 1. The varistor voltage is a voltage corresponding to a current of the varistor of 1 mA, and is a standard of a voltage whose current rapidly rises with voltage, and the voltage is expressed by $U_{1mA}$. The leakage current refers to the current flowing through the varistor at a specified temperature and maximum DC voltage, generally expressed by $I_{ie}$. Under the premise of approaching $U_{1mA}$, the smaller the $I_{ie}$ was, the better the voltage limiting performance of the varistor would be. In this study, 7 ZnO varistor blocks, with the majority approaching the static parameters, were selected as the samples, and were denoted as A1 to A7.

Preprints (www.preprints.org) | NOT PEER-REVIEWED | Posted: 18 January 2019 doi:10.20944/preprints201901.0183.v1

Peer-reviewed version available at Electronics 2019, 8, 172; doi:10.3390/electronics8020172

**Table 1** Changes in the electrical parameters before and after the impulse of ZnO varistors

| No. | Initial $U_{1mA}$ (V) | Initial $I_{ie}$ (μA) | $U_{1mA}$ when failure (V) | $I_{ie}$ when failure (μA) | $T_{max}$ when failure (°C) | Groups of impulse |
|---|---|---|---|---|---|---|
| A1 | 690 | 0 | 602 | 8.2 | 224 | 17 |
| A2 | 689 | 0 | 600 | 8.1 | 225 | 16 |
| A3 | 690 | 0 | 604 | 7.5 | 222 | 15 |
| A4 | 691 | 0.1 | 615 | 9.4 | 221 | 16 |
| A5 | 688 | 0.1 | 605 | 8.6 | 216 | 16 |
| A6 | 690 | 0.1 | 603 | 8.5 | 228 | 15 |
| A7 | 689 | 0.1 | 602 | 7.8 | 218 | 16 |

### 2.3 Experimental procedure

The flowchart of the experimental procedure is shown in Fig. 4.

Preprints (www.preprints.org) | NOT PEER-REVIEWED | Posted: 18 January 2019 doi:10.20944/preprints201901.0183.v1

Peer-reviewed version available at Electronics 2019, 8, 172; doi:10.3390/electronics8020172

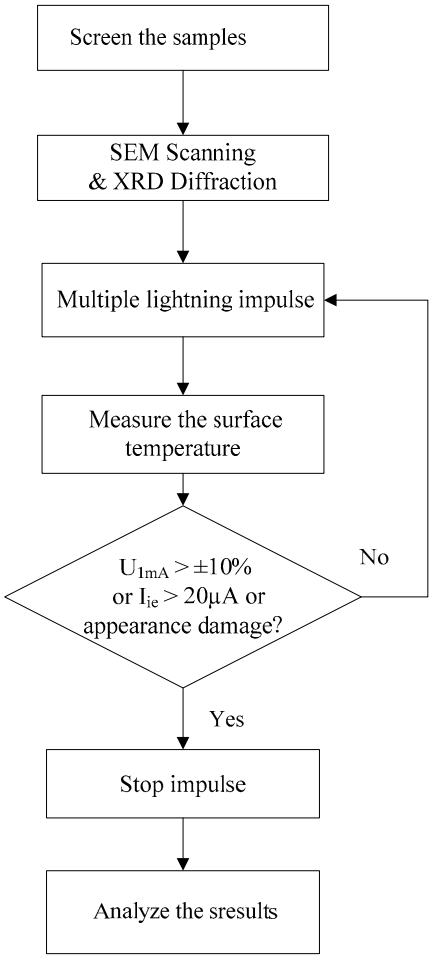


**Fig. 4** Flowchart of the experimental procedure.

(1) Initial measurements: The samples are characterized with the $U_{1mA}$, $I_{ie}$ and photographs at the beginning of the test.

(2) Impulse test: We adjusted the charging voltage of the generator to output the demand impulse currents. Then, multiple lightning impulse currents were applied to the ZnO varistors. The time between the application of one group of impulse current to a ZnO varistor block and that of the next group of impulse current was 30 minutes; with such long duration of time, we were able to recover to the original conditions. The process of the impulses is shown in Fig. 5. When the change

Preprints (www.preprints.org) | NOT PEER-REVIEWED | Posted: 18 January 2019 doi:10.20944/preprints201901.0183.v1

Peer-reviewed version available at Electronics 2019, 8, 172; doi:10.3390/electronics8020172

amplitude of the $U_{1mA}$ reached beyond ±10% of the original, the $I_{ie}$ exceeded 20 μA, or direct damage occurred, the ZnO varistors were judged as having failed. Subsequently, the impulse test was ceased, and the data were recorded.

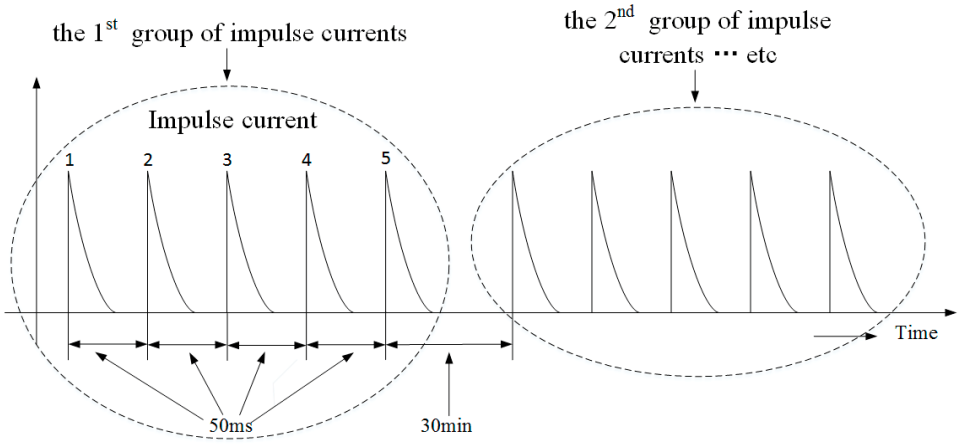


**Fig. 5** Groups of impulse current applied to ZnO varistors.

(3) We measured the surface temperatures, varistor voltage $U_{1mA}$ and leakage current $I_{ie}$ of the ZnO varistors after each impulse. Then we checked the surface of the ZnO varistors for flashover or puncture, and took photographs of the damaged ZnO varistors.

(4) We used scanning electron microscopy (SEM) and X-ray diffractometer (XRD) on the ZnO varistor block before and after the impulse in order to observe the microscopic structures of the ZnO varistors.

## 3 Results and discussion

### 3.1 Macroscopic property

The average level change directions of the $U_{1mA}$ and $I_{ie}$ after the increases in the impulse groups for the ZnO varistors under multiple lightning impulse current can be seen in Fig. 6. It can be observed

Preprints (www.preprints.org) | NOT PEER-REVIEWED | Posted: 18 January 2019 doi:10.20944/preprints201901.0183.v1

Peer-reviewed version available at Electronics 2019, 8, 172; doi:10.3390/electronics8020172

that the $U_{1mA}$ showed a trend of decreasing-stable-decreasing with the increases of impulse groups, which was observed to drop after the first group of impulse and the last group of impulse with an average decline rate as high as 4%. The $I_{ie}$ all showed increasing trends with larger rising rates, with an average growth rate of 0.66 μA/a group. Following the 16 groups of impulse, it was observed that the $U_{1mA}$ fell sharply, with an average drop rate of more than 10% of the original $U_{1mA}$. This resulted in failures occurring in the ZnO varistors. Then, after another group of impulses, the ZnO varistor blocks became damaged.

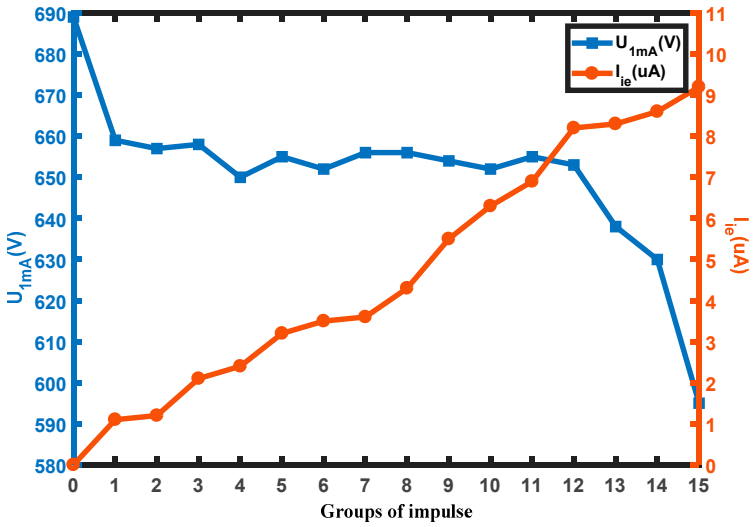


**Fig. 6** Varistor voltage $U_{1mA}$ and leakage current $I_{ie}$ variation diagrams of the ZnO varistors under multiple lightning impulse current.

As shown in Table 1, under the five-pulse lightning current, the ZnO varistor blocks A1 to A7 were able to withstand an average of 16 groups of impulse. When the $U_{1mA}$ had fallen by more than 10% of the initial value, the appearance of damages occurred in the cases of a maximum of 1 to 2 groups of impulses. Figure 7(b) shows the damage forms of the ZnO varistor block A2 during its failure, which presented a side-corner cracking along with patch collapse [21]. As shown in Fig.

Preprints (www.preprints.org) | NOT PEER-REVIEWED | Posted: 18 January 2019 doi:10.20944/preprints201901.0183.v1

Peer-reviewed version available at Electronics 2019, 8, 172; doi:10.3390/electronics8020172

7(c), the damage forms of the ZnO varistor blocks A1 to A4 in the different codes were observed to be highly consistent.

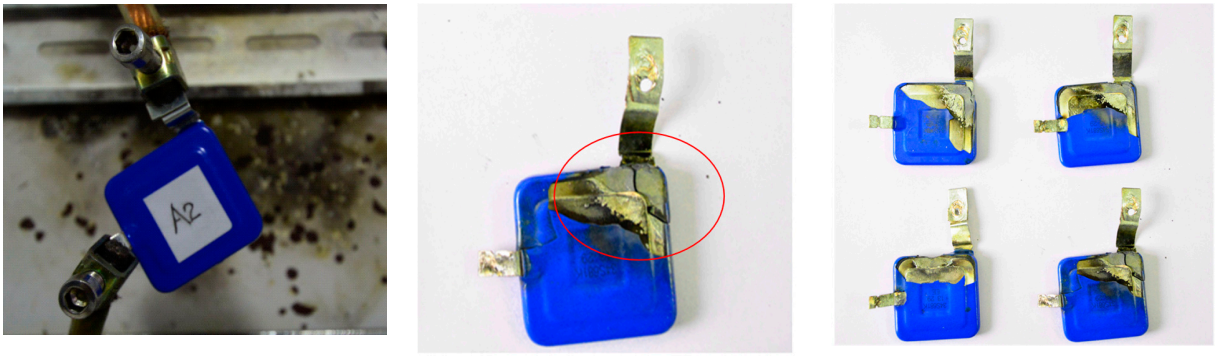


**(a)** **(b)** **(c)**

**Fig. 7** Appearance state diagram of the ZnO varistors before and after the multiple lightning impulse current. **(a)** State diagram of Sample A2 before impulse. **(b)** Damage state diagram of Sample A2. **(c)** Damage diagrams of Samples A1 to A4.

### 3.2 Microscopic property

Figure 8 details the SEM images of the ZnO varistors prior to the impulses with a resolution of 10 μm. It can be seen from the figure that the internal structure of the ZnO varistor was mainly composed of four types of gray matter, marked as +1, +2, +3, and +4, respectively. Through this study's EDS analysis, it was determined that the main components of +1 in the white area were O, Zn, and Bi; those of +2 in the gray area were O and Zn; those of +3 at the white-gray junction were O, Zn, and Bi, and those of +4 in the deep black region were O and Zn. The proportion of elements in different regions was shown in Fig. 8(b). It could be seen that the main components of the ZnO varistor were zinc oxide, and small amounts of Bi compounds. The gray area in the figure indicated the zinc oxide grain, and the white area indicates the rich-Bi phase included around the

Preprints (www.preprints.org) | NOT PEER-REVIEWED | Posted: 18 January 2019 doi:10.20944/preprints201901.0183.v1

Peer-reviewed version available at Electronics 2019, 8, 172; doi:10.3390/electronics8020172

zinc oxide grain. It was found that the cell distributions of the ZnO varistor were not uniform, and the rich-Bi phase was concentrated in a certain region. Map analysis at +1 position of the ZnO varistors was shown in Fig. 8(c).

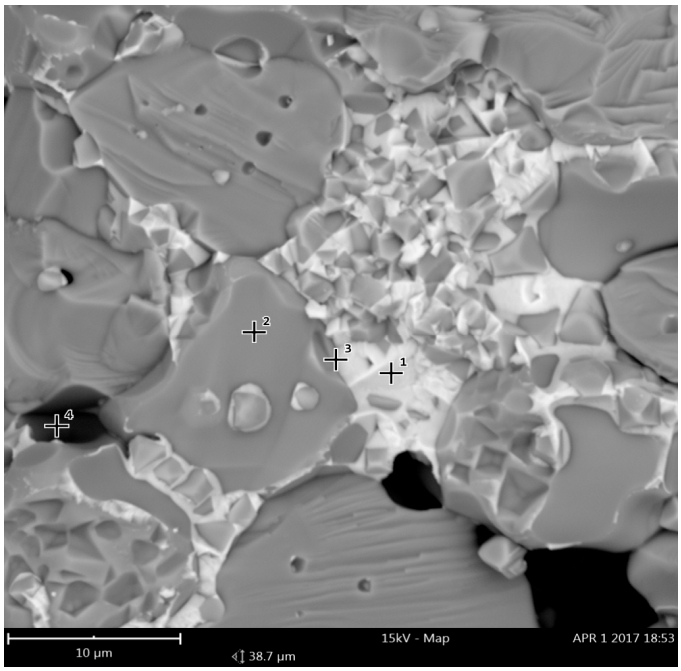


**(a)**

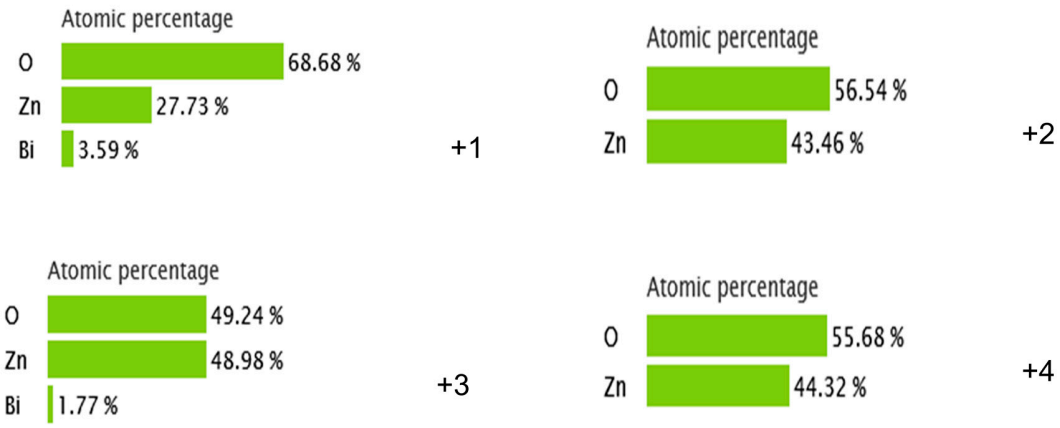


**(b)**

Preprints (www.preprints.org) | NOT PEER-REVIEWED | Posted: 18 January 2019 doi:10.20944/preprints201901.0183.v1

Peer-reviewed version available at Electronics 2019, 8, 172; doi:10.3390/electronics8020172

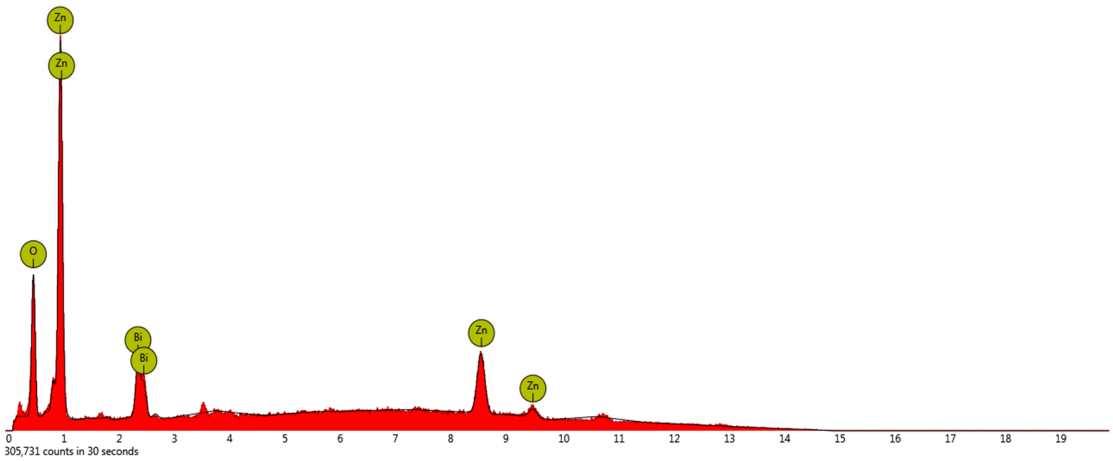


**(c)**

**Fig. 8 (a)** SEM images of the ZnO varistors (resolution of 10 μm). **(b)** EDS analysis results of the ZnO varistors. (+1, +2, +3, +4). **(c)** Map analysis at +1 position of the ZnO varistors.

Figures 9(a) and 9(b) shows the XRD diffraction pattern of the ZnO varistors before and after the impulses. It can be seen in the figure that the crystal phase compositions mainly included four parts as follows: Zincite, syn; Manganese Oxide; Bismuth oxide; Bismite, syn. Through the analysis of the figures, it was determined that the proportion of Bi in the several crystal phases before the impulse test was 0.9%, 0.8%, and 0.6%, respectively. The proportion after the impulse test was 0.0%, 1.0%, and 1.3%, respectively. The proportion of Bi in several crystal phases has been converted.

Preprints (www.preprints.org) | NOT PEER-REVIEWED | Posted: 18 January 2019 doi:10.20944/preprints201901.0183.v1

Peer-reviewed version available at Electronics 2019, 8, 172; doi:10.3390/electronics8020172

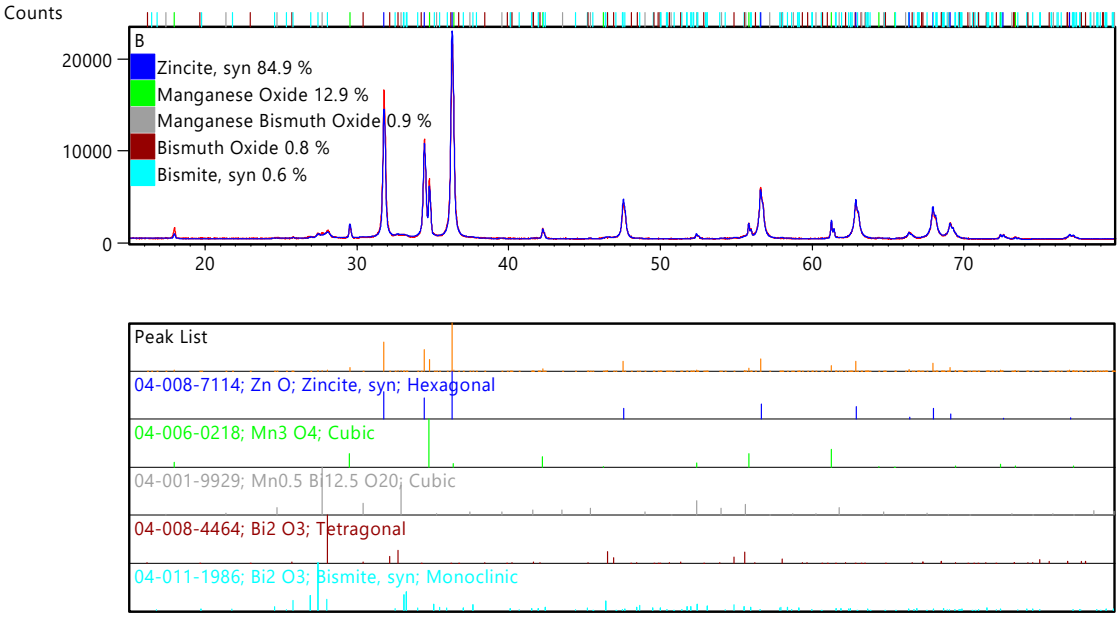


**(a)**

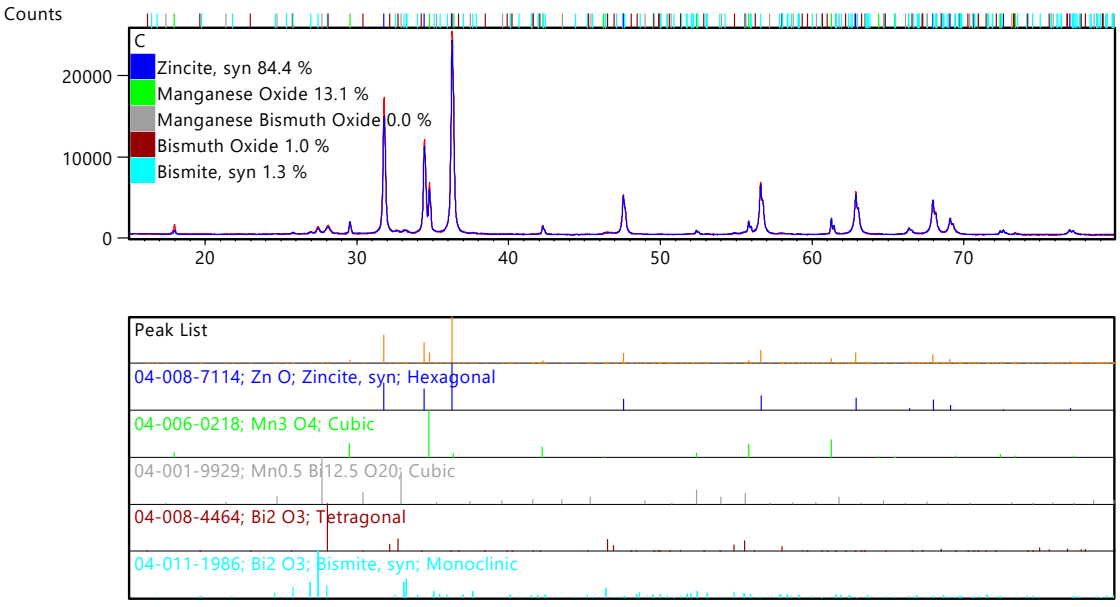


**(b)**

**Fig. 9** XRD diffraction results of the ZnO varistors before **(a)** and after **(b)** the impulses.

Preprints (www.preprints.org) | NOT PEER-REVIEWED | Posted: 18 January 2019 doi:10.20944/preprints201901.0183.v1

Peer-reviewed version available at Electronics 2019, 8, 172; doi:10.3390/electronics8020172

Figures 10(a) and 10(b) illustrate the SEM images of the ZnO varistors before and after the impulses with a resolution of 80 μm. It was observed that, after the impulses, the grain sizes became smaller, while the white areas increased. The differences in the microstructures of the ZnO varistors' material indicated that the multiple lighting impulse currents had led to the ZnO grains becoming smaller along with the grain boundary growth.

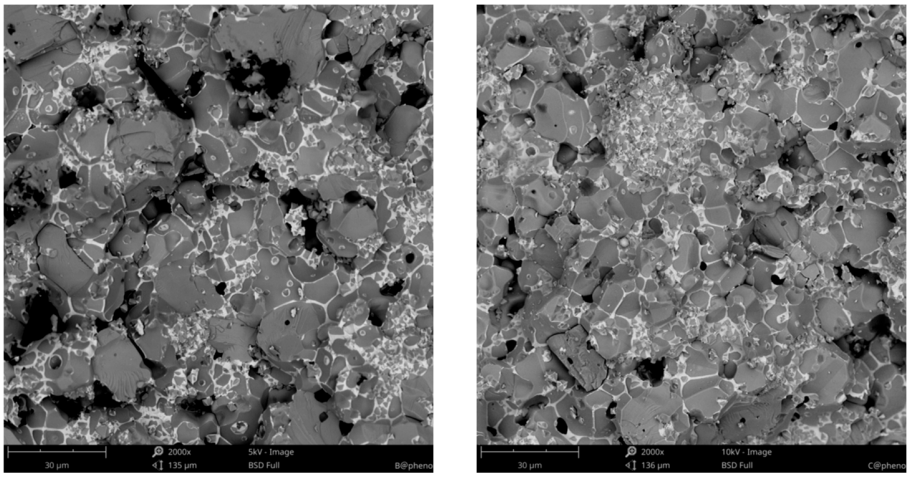

**(a)** **(b)**

**Fig. 10** SEM images of the ZnO varistors (resolution of 80 μm). **(a)** Before the impulses. **(b)** After the impulses.

### 3.3 Failure mechanism

The appearance of the ZnO varistors resembles layers of insulation coating. When a single impulse current passes the ZnO varistors in the time of a subtle order of magnitude, the pulse intervals are ms in length, and the internal heat of ZnO varistors will be almost instantaneously concentrated, accompanied by a sharp rise in temperature. In terms of the energy convection and exchange, this process can be seen as an adiabatic temperature rise. When the failures occurred in the ZnO

Preprints (www.preprints.org) | NOT PEER-REVIEWED | Posted: 18 January 2019 doi:10.20944/preprints201901.0183.v1

Peer-reviewed version available at Electronics 2019, 8, 172; doi:10.3390/electronics8020172

varistors, the surface temperature rose to over 200°C, and the average temperature was 223°C, as shown in Table 1. According to Eq. (1), in the cases of the injected energy equivalent, the temperature rises of the ZnO varistors units with the intake of energy could be directly determined by the thermal physical property parameters ρ and Cp of the ZnO varistors. However, during the production process of the ZnO varistors, the absolute equality of the material mixing uniformity could not be achieved. As viewed from the SEM images of the ZnO varistor block, the microstructures showed the inhomogeneities of the internal material distribution, which were observed to have led to significant differences in the thermal physical properties of the same ZnO varistors at different parts. For example, inhomogeneities existed in the thermal physical properties of the ZnO varistor block. It was determined in this study that the ρ and Cp differences at different parts led to different adiabatic temperature rises. Furthermore, the infrared imaging measurement results showed different temperature rises in the different locations of ZnO varistor block after absorbing the impulse energy. Figure 11 shows the temperature distribution diagram of the ZnO varistor block A1 and A4 following the impulses. It can be seen in the figure that there were considerable differences observed in the temperature rises at different parts. The energy at the local hot spot occurred too late to pass around, which led to a large temperature gradient between the hot spot and the surrounding area. Thermal stress to the temperature gradient occurred in the interior of the ZnO varistor block. When the thermal stress reached a certain value, it caused burst damages to the ZnO varistor block [22].

Preprints (www.preprints.org) | NOT PEER-REVIEWED | Posted: 18 January 2019 doi:10.20944/preprints201901.0183.v1

Peer-reviewed version available at Electronics 2019, 8, 172; doi:10.3390/electronics8020172

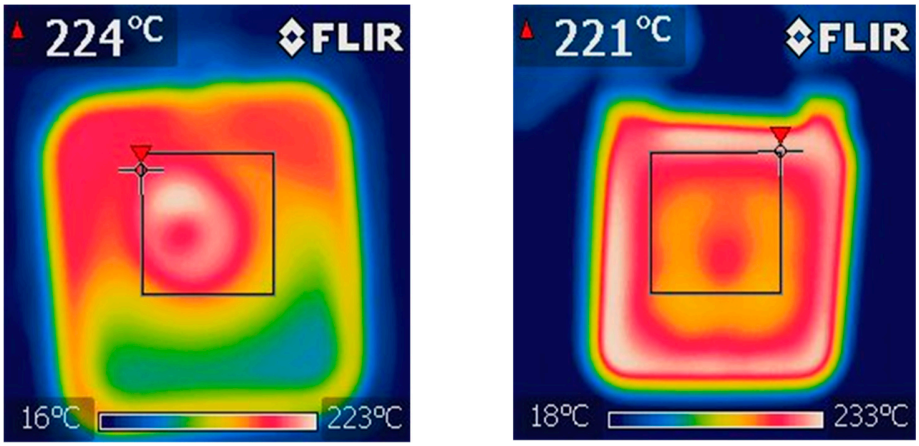


**(a)** **(b)**

**Fig. 11** Temperature distribution map of the ZnO varistor after impulses. **(a)** Varistor block A1. **(b)** Varistor block A4.

The adiabatic temperature rises of the ZnO varistor units after the absorption of energy $W$ (unit: J) were as follows:

$$\Delta T = \frac{\Delta W}{\Delta V \rho c_p} \tag{1}$$

In Fig. 11, $\Delta V$ is the volume of the ZnO varistors unit; $\rho$ is the proportion of the ZnO varistors with an average of 5,600 kg/m$^3$; and $C_p$ is the constant-pressure heat capacity of the ZnO varistors units, which was approximately 500 J/kg·°C at 20°C.

If the temperature rises of the adjacent two units were $\Delta T_1$ and $\Delta T_2$, respectively, then the thermal stress $f$ under the effects of the temperature gradient was as follows:

$$f = \frac{E\mathrm{a}}{1-\mu}(\Delta T_1 - \Delta T_2) \tag{2}$$

Where $E$ is the elastic modulus; a denotes the thermal expansion coefficient; and $\mu$ is the Poisson's ratio. When the thermal stress $f$ produced under the action of the temperature gradient

Preprints (www.preprints.org) | NOT PEER-REVIEWED | Posted: 18 January 2019 doi:10.20944/preprints201901.0183.v1

Peer-reviewed version available at Electronics 2019, 8, 172; doi:10.3390/electronics8020172

exceeded the thermal stress threshold during the rupture failure of the ZnO varistors material, it could potentially lead to the destruction of the ZnO varistors.

The experimental phenomenon in which the varistor voltage presented a declining trend could be explained by the microstructure characteristics of the ZnO varistors. As shown in Fig. 10, the SEM images confirmed that the interiors of the ZnO varistors were composed of many zinc-oxide grains, and the distances between various grains were fixed. Meanwhile, transverse and longitudinal capacitances were formed between the grains, which displayed a vertical distribution.

The microanalysis showed that the grain sizes of the ZnO varistors became smaller, while the area of the grain boundary layer increased, which led to the increases in the capacitance of the grain boundary layer as follows:

$$C = \frac{\varepsilon S}{4\pi kd} = \frac{Q}{V} \tag{3}$$

In Eq. (3), C represents the capacitance; ε is the dielectric constant; S is the cross-sectional area; k denotes the electrostatic force constant; d is the anode-to-cathode distance; Q represents the charge quantity; and V is the voltage.

It can be seen from the above equation that, as the number of impulse groups increased, the capacitance of the grain boundary layer increased, while the varistor voltage gradually decreased.

Following the ZnO varistors under the multiple lightning impulse current, the leakage current value gradually increased. This was due to the fact that after several impulse groups, the ZnO varistors absorbed the impulse energy, and the temperatures rose. This speeded up the rates of the ion migration, resulting in the leakage current values displaying a growing trend.

Preprints (www.preprints.org) | NOT PEER-REVIEWED | Posted: 18 January 2019 doi:10.20944/preprints201901.0183.v1

Peer-reviewed version available at Electronics 2019, 8, 172; doi:10.3390/electronics8020172

## 4 Conclusions

In this study, the experiments were conducted to investigate the microstructure and macroscopic properties of the ZnO varistors under multiple lightning impulse current.

(1) The macroscopic failure mode of ZnO varistors under multiple lightning impulse could be described as the electrical parameters deterioration rapidly with the increase of the number of impulse groups, and finally destroyed by side-corner bursting. Under a five-pulse lightning current, the ZnO varistors were able to withstand an average of 16 groups impulse.

(2) The microstructural examination indicated that after the multiple lightning strokes, the proportion of Bi in the several crystal phases has been converted, the grain size of the ZnO varistors became smaller, and the white intergranular phase (Bi-rich grain boundary layer) increased significantly.

(3) The ZnO varistors undergoing multiple lightning impulse currents presented adiabatic temperature rises. It was observed that, due to the unevenness of the material, the ZnO varistors displayed local temperature rises after absorbing impulse heat. The failure mechanism is thermal damage and grain boundary structure damage caused by temperature gradient thermal stress generated by multiple lightning currents.

## Acknowledgements

This study is financially supported by the National Nature Science Foundation of China (NSFC Grants No. 61671248) and Open Foundation of Jiangsu Key Laboratory of Meteorological Observation and Information Processing (KDXS1603) and A Project Funded by the Priority Academic Program Development of Jiangsu Higher Education Institutions (PAPD). The authors are thankful to the anonymous reviewers for their valuable comments.

Preprints (www.preprints.org) | NOT PEER-REVIEWED | Posted: 18 January 2019 doi:10.20944/preprints201901.0183.v1

Peer-reviewed version available at Electronics 2019, 8, 172; doi:10.3390/electronics8020172

## References

[1] He J H, Liu J, Hu J, et al. Development of ZnO varistors in metal oxide arrestors utilized in ultra high voltage systems. High Voltage Engineering, 2011, 37(3): 634–643

[2] He J, Yuan Z, Wang S, et al. Effective protection distances of low-voltage SPD with different voltage protection levels. IEEE Transactions on Power Delivery, 2010, 25(1): 187–195

[3] British Standards Document. Low-voltage surge protective devices. Surge protective devices connected to low-voltage power systems. Requirements and test methods. 2011, IEC61643-11

[4] Ringler K G, Kirkby P, Erven C C, et al. The energy absorption capability and time-to-failure of varistors used in station-class metal-oxide surge arresters. IEEE Transactions on Power Delivery, 1997, 12(1): 203–212

[5] Takada M, Yoshikado S. Effect of $SnO_2$ addition on electrical degradation of ZnO varistors. Key Engineering Materials, 2007, 350: 213–216

[6] de Salles C, Martinez M L B, de Queiroz A A A. Ageing of metal oxide varistors due to surges. In: 2011 International Symposium on Lightning Protection: IEEE, 2011, 171–176

[7] Tsukamoto N. Study of degradation by impulse having 4/10μs and 8/20μs waveform for MOVs (metal oxide varistors). In: 2014 International Conference on Lightning Protection (ICLP): IEEE, 2014, 620 – 623

[8] Bassi W, Tatizawa H. Early prediction of surge arrester failures by dielectric characterization. IEEE Electrical Insulation Magazine, 2016, 32(2): 35–42

Preprints (www.preprints.org) | NOT PEER-REVIEWED | Posted: 18 January 2019 doi:10.20944/preprints201901.0183.v1

Peer-reviewed version available at Electronics 2019, 8, 172; doi:10.3390/electronics8020172

[9] Matsumoto Y, Sakuma O, Shinjo K, et al. Measurement of lightning surges on test transmission line equipped with arresters struck by natural and triggered lightning. IEEE Transactions on Power Delivery, 1996, 11(2): 996–1002

[10] Zhang Q L, Qie X S, Kong X Z, et al. Comparative analysis on return stroke current of triggered and natural lightning flashes. Proceedings of the CSEE, 2007, 27(6): 67–71

[11] Heidler F, Zischank W, Flisowski Z, et al. Parameters of lightning current given in IEC 62305-background, experience and outlook. In: 29th International Conference on Lightning Protection, Uppsala, Sweden, 2008, 26

[12] Darveniza M, Tumma L R, Richter B, et al. Multipulse lightning currents and metal-oxide arresters. IEEE Transactions on Power Delivery, 1997, 12(3): 1168–1175

[13] Lee B-H, Kang S-M. Properties of ZnO varistor blocks under multiple lightning impulse voltages. Current Applied Physics, 2006, 6(5): 844–851

[14] Lee B-H, Kang S-M, Pak K-Y, et al. Effect of multiple lightning impulse currents on Zinc oxide arrester blocks. In: Proceedings of the 27th International Conference on Lightning Protection, Avignon, France: The Korean Institute of Electrical Engineers, 2004, 634–639

[15] Haryono T, Sirait K T, Tumiran T, et al. The damage of ZnO arrester block due to multiple impulse currents. TELKOMNIKA (Telecommunication Computing Electronics and Control), 2011, 9(1): 171

[16] Haryono T, Sirait K T, Tumiran T, et al. Effect of multiple lightning strikes on the performance of ZnO lightning arrester block. High Voltage Engineering, 2011, 37(11): 2763–2771

Preprints (www.preprints.org) | NOT PEER-REVIEWED | Posted: 18 January 2019 doi:10.20944/preprints201901.0183.v1

Peer-reviewed version available at Electronics 2019, 8, 172; doi:10.3390/electronics8020172

[17] Vahidi B, Cornick K, Greaves D. Effects of multiple stroke on ZnO surge arresters. In: Proceedings of the 24th International Conference on Lightning Protection, Binningam, England, 1998, 960–963

[18] Heinrich C, Wagner S, Richter B, et al. Multipulse tests on surge arresters for medium and low voltage systems. In: Proceedings of the 24th International Conference on Lightning Protection, Birmingham, England, 1998, 790–794

[19] Munukutla K, Vittal V, Heydt G T, et al. A practical evaluation of surge arrester placement for transmission line lightning protection. IEEE Transactions on Power Delivery, 2010, 25(3): 1742–1748

[20] International Electrotechnical Commission. Protection against lightning – Part 1: General priciples. 2006, BS EN/IEC 62305-1

[21] Darveniza M, Mercer D R. Laboratory studies of the effects of multipulse lightning currents on distribution surge arresters. IEEE Transactions on Power Delivery, 1993, 8(3): 1035–1044

[22] Wu W H, He J L, Gao Y M. Impact damage principle of metal oxide valve plates. In: Properties and Applications of Nonlinear Metal Oxide, Varistors, 5nd ed. Beijing, China: Tsinghua University Club, 1998, 147–149